OPEN ACCESS
*World Journal of Multidisciplinary Studies*
ISSN (Online): 3049-0855 | Vol. 3, No. 3, Mar. 2026
Website: https://wasrpublication.com/index.php/wjms

# Arc-Tangent Algorithm for anti-jamming of the GALILEO signals

**Yamuna Sharma[1], Tamesh Halder[2*], Arindam Basak[1], Sarita Nanda[1], Debashish Chakravarty[2]**

[1] School of Electronics Engineering KIIT, Bhubaneswar 751024, India

[2] Dept. of Mining Engineering IIT Kharagpur, Kharagpur-721302, India.

Received: 20/12/2025 | Accepted: 07/02/2026 | Published: 21/03/2026

**Abstract:** Due to the diversified applications, GPS i.e Global Positioning System is the most widely used navigation system till date. However, in itself it consumes a number of flaws in terms of accuracy. Later on, with the development of the Global Navigation Satellite System (GLONASS) was designed to overcome these issues, however it failed to meet expectations. Galileo GNSS was the most current and sophisticated development in 2016, and it was released in 2016. It is the most recent satellite navigation system, with higher tracking speed and accuracy superior to both the earlier systems, GPS and GLONASS. This study aims to construct chirp jamming to jam the acquisition signal, then anti-jamming the Galileo GNSS signal using ATSA and ATLMS algorithm to recover the signal that is being provided as an input, which is unavailable in any of the navigation literatures till now. Basically, the objective of the paper is to describe the two arc tangent algorithms, i.e, Arc-tangent Sign Algorithm and Arc-tangent Least Mean Square Algorithm. It is the MATLAB-based simulation for supervising the mitigation techniques using the arc Arc-tangent algorithms. GALILEO signals, their transmission, and reception techniques are also described in the paper.

**Keywords**: ATSA, ATLMS, Arc-Tangent, Galileo, Anti-Jamming.

## 1 Introduction

The Global Positioning System (GPS) made us forget the compass of the olden days. As radio-navigational satellite systems upgrade, interest in next-generation signals and systems for civilian use is growing. In today's telecommunications, significant worldwide global-navigation satellite systems (GNSS) such as GPS, GALILEO, GLONASS, and Compass have all been introduced and have advanced rapidly. [1]

In the case of substantial interference, the crowded allotted frequency bands of satellites of various navigational satellite systems cause technical and receiver performance challenges. [2] Due to multipath and fading, satellite navigation receivers always have poor signals. In the next generation of systems, signal design requires the mitigation of multipath fading and interference. The receiver design should also be enhanced to address signal acquisition and tracking issues. The need for interference mitigation or anti-jamming for obtaining data reliably utilizing the GNSS receiver mechanism is extensively discussed in the paper. Only a few GPS anti-jamming systems for receivers have been developed in the previous decade, [3] aside from military applications, to improve the process of information retrieval.

A lot of pre-correlation and post-correlation systems have been developed to improve signal quality, but they require complicated circuitry and are thus not cost-effective in some circumstances. As a result, the GNSS has been instrumental in furthering the interests of scholars all over the world. The GALILEO signals incorporate all advanced features seen in contemporary GNSS, such as multiple frequency transmission, secondary codes, and pilot components, as well as use of greater power levels, wide bandwidths, and error correction codes, are included in the GALILEO signals. Faster chip speeds, wider pseudo-noise codes, and modulation schemes and variations of the Binary Offset Carrier (BOC) [4] are among the other characteristics.

Despite being the world's oldest navigation technology, GPS is not without its flaws. It is not the fastest navigation method since information is relayed with some lag. The GPS's positional tracking accuracy is only good for five meters, but current applications need more precision. So, GLONASS which was developed by Russia in the mid-1980s helped improve tracking accuracy marginally. It was shown to be somewhat quicker than GPS, however, this was owing to its proximity to the earth's surface. [2] GALILEO GNSS is the most modern navigation technology to successfully handle the majority of these issues. GALILEO's tracking precision is one meter, which is far better than prior systems like GPS. It gives precise readings for greater latitudes and is speedier at conveying the pieces of information.

The BOC modulation scheme was initially suggested in late 2004 and has since been updated to set up on the L1 frequency band, accompanied by the GALILEO Open Service (OS) on the E1 frequency band.[5] It's a novel modulation approach that grants BOC in the E1 or L1 frequency bands while avoiding interference with the GPS or GALILEO systems. The Composite Binary Offset Carrier (CBOC) which is a form of Multiplexed Binary Offset Carrier (MBOC), its Power Spectral Density (PSD) has more high-frequency components, which help the system function better in terms of tracking precision and multipath compatibility. However, there are several limitations, such as the Auto Correlation Function's (ACF) many lateral peaks, which cause several puzzling issues. Many acquisition techniques have been introduced to eliminate these problem-causing side peaks, such as pseudo-BPSK, [6] pseudo correlation function (PCF), [7,8] and subcarrier phase

***Corresponding Author**
**Tamesh Halder***
Dept. of Mining Engineering IIT Kharagpur, Kharagpur-721302, India.

cancellation (SCPC), [9] but the majority of these strategies are expressed for such BOC signal, and as for other forms such as MBOC [10] or CBOC are difficult to jam.

Interference-related distress is a key source of concern for navigation-related systems. Because the idea of distributed spectral energies in particular frequency regions, which is prominent in the modern navigation techniques and it also produces jammer-attenuation, anti-jamming approaches are not as effective as in lower to moderate interference systems. When the level of interfering power rises, navigation systems require the use of anti-jamming solutions. Implementation of the anti-jamming algorithms for GPS Signals is being noticed in a few of the literature, but for the GALILEO Signals, implementation of the anti-jamming algorithm provides a new angle to this literature. The uniqueness of this research is the implementation of the ATLS (Arctangent Sign Algorithm), and ATLMS (Arctangent Least Mean Square) algorithms for anti-jamming the acquisition signal of GALILEO GNSS.

The other sections of the paper are arranged as follows: the second portion follows up with the further explanation of the GALILEO signals its positioning techniques and the services provided by it, the third one explains the techniques and details the system setup, the fourth section briefs the algorithm used in the simulations for anti-jamming the acquired signal. The fifth section examines the simulation results and the last portion concludes the entire literature and ends the study.

The primary goal of utilizing GPS or GNSS is to get the user's location, velocity, and time (PVT) concerning a reference frame. [11] We need three satellites for coordination and another one for clock bias for measuring the range. It is possible to detect the phase of an incoming signal by comparing it to the 'local receiver produced replica.' With four satellites and their known distances from Earth, one may determine longitude, latitude, altitude, and the user's clock bias adjustment. The essential method for determining the PVT is 'trilateration,' and the receiver must use at least four satellites to solve the so-called 'navigation equation' for position-related data. The Doppler shift in the received signal may also be used to estimate the user's relative velocity.

Galileo signals incorporate all of the contemporary features seen in current GNSS, such as multiple frequency transmission, pilot components and secondary codes and as well as the use of wide bandwidth, low power level and error correction codes. Other characteristics include faster chip speeds, lengthier pseudo-noise codes and modulations such as BOC and MBOC and the variations thereof. Hence the design of the GALILEO Signals is discussed in the following sections.

## 2 Techniques and the Architecture

One or more spreading sequences that are modulated on carrier signals are one of the navigation signal components. Various spreading codes and data are modulated on the same carrier for each navigation signal. A signal's spreading code denotes a single Pseudo-Random Noise (PRN). The signal bandwidth expands when the signal is modulated using a high rate PRN code. Because of this, the PRN code is also known as the spreading code. Chip duration Tc refers to the shortest transition time interval in distributing code. It highlights the benefits and the drawbacks of various modulation schemes, as well as the superiority of Multiplexed Binary Offset Carrier (MBOC) [4] modulation over others. MBOC modulated signal is the outcome of adding or multiplexing in the time domain of two or more BOC signals [12].

### 2.1 Architecture of the Transmitter

In GPS, C/A code, also known as the Civilian Acquisition or Access Code, is modulated with navigation data. C/A code computes half of the frequency of C/A navigation, which is 1.023 MHz. The navigation data signal is 50 Hz. Furthermore, the resultant signal is a BPSK modulated signal with an addition of a carrier signal. A separate PRN code is provided for every satellite in the GPS constellation. Changing the G2 register connection might result in the creation of distinct PNR signals, i.e. the LFSR receiving various inputs.

Because of MBOC modulation, the architecture of the GALILEO transmitter is more complicated than any other topologies. Both forms of modulated signals, Composite BOC and Time MBOC, have been implemented, where the generated modulated signals are being multiplied with the carrier signal. After that, the carrier modulated signal is subsequently broadcast through the channel.

The E1 band is used by the GALILEO system, with a central frequency of 1575.42 MHz. Code length of the GALILEO signal is 4092 chips, which is roughly four times longer than the length of C/A code of GPS. On an Intermediate frequency (IF) simulator, MBOC signals and the IF carrier signal are supplied, and the needed sampling frequency is determined by wideband or narrowband processing done on the receiver. The sampling frequency should be properly chosen. Signal synchronization is strongly dependent on the sampling frequency, and the optimal oscillator frequency created is known to be exact.

### 2.2 Architecture of Receiver

A receiver is a device that processes the signal transmitted by GALILEO satellites to determine a navigation solution. It is used to catch and isolate RF signals from satellites. To decode navigation signals and grasp the PVT, Position, Velocity and Time for users and satellites, readings of the Doppler shift and signal sync are taken in the receiver region. Time based surveys or differential surveys are also performed. A reference oscillator, antenna, frequency synthesizer, IF section, pre-amplifier, signal processing, and application processing and positioning are the essential elements of the receiver design. The Signal Processing toolbox in the IF Section stores and runs the method for anti-jamming GALILEO signals. This algorithm understands the PVT and obtains the signal. The received signal must be distorted since it may be integrated with other signals, mostly noise. Thus anti-jamming algorithms are utilized to remove noise from the received signal. Fig (1) depicts the diagrammatic representation of typical radio receiver architecture.

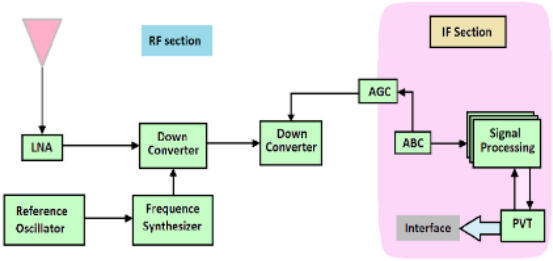


Fig 1 :- Representation of the receiver's architecture

At first, the antenna component converts the incident wave's electric field to a different signal that is an electric power signal. The antenna layout is globular in order to follow satellites first from the zenith to the horizons. LNA termed as Low Noise Amplifier follows the antenna, which is either RHCP, right-hand circular polarized or LHCP, left-hand circular polarized that fit the input signals and excludes the reflected signals. The preamplifier really comprises LNA, filtering and burnout prevention procedures to offer a lower noise figure and out-of-band interference rejection. Down conversion and Analog to Digital conversion are included under the Radio Frequency (RF) section, which deals with high frequencies. A mixer-associated frequency synthesizer and a local oscillator are typically used in frequency down-conversion. In this part, filtering is a necessary operation.

To acquire the IF signal a homodyne receiver architecture requires just one down-conversion whereas a heterodyne requires two or more down-conversions. The majority of GNSS receivers employ either a zero-IF design with a homodyne configuration or the architecture of super heterodyne with two subsequent down conversions. The local oscillator in a GNSS receiver [13] plays a important role in exhibiting frequency flexibility for dealing with Doppler frequencies and ideal code velocity in considerations of code values for improved correlations. The ADC digitizes the IF signal utilizing, AGC, Automatic Gain Control after the down-conversion [14]. Then it is being integrated by the digital signal processing (DSP) component.

The hemispheric antenna design allows satellites to be tracked from their zenith to their horizons. The low noise amplifier comes after the antenna (LNA). Filtering, LNA, and a burnout prevention mechanism make up the pre-amplifier, which provides low noise and band rejection. In the radio frequency section, a section that deals with higher frequency components which contains the descending version and analog to digital, A-D conversion. Frequency synthesizer and local oscillator connected with the mixer are frequently used for frequency down-conversion. Filtering is a crucial operation in this part.

To create the MBOC receivers, firstly, we employ the architecture of software-defined recipients. The SDR idea is innovative, and simulation or emulation can be used to create and handle SDR's dynamic properties. [15] Previously, the complicated hardware design was too rigid for configuration. Since the late 1970s, the SDR has operated in the defense industry in the United States and Europe. Speak Easy, a US military communication effort, was the name of this program. A versatile DSP platform is provided by radio software-defined technology. [16] This may be done with the computers or other machines that supports the use of some softwares such as MATLAB, [17] LAB VIEW, and others, or with FPGAs, ASICs, and enabled microprocessors, but the physical implementation is less reversible.

## 2.3 Front End Filter

Front-end filter is positioned in between the acquisition unit of the receiver and the channel model. The filter is explained in the following lines. The front-end filter [18] has a narrow bandwidth of 4 MHz and a double-sided bandwidth. In this situation, a Chebyshev type I filter of order 6 is utilized with a 3-dB double-sided bandwidth of 4 MHz. Front filters with a double-sided bandwidth of 16 MHz (ideal for wide-band receivers) - A Chebyshev type I filter with order 4 and a 3-dB double-sided bandwidth of 16 MHz is utilized. The acquisition unit can use the front-end filter output directly

## 2.4 Acquisition Unit

Popular acquisition techniques for navigational purposes include Parallel acquisition in the Doppler frequency domain, serial search technique, and parallel acquisition in the time-delayed domain. The main goals of this unit are to identify PRN and to estimate certain values from the noisy signal, that is, the code phase and the doppler frequency [19] obtained at receiver by comparing it to the PRN code produced locally or by the receiver. Our receiver acquisition unit uses Fast Fourier Transform, FFT correlating the local replications and the received signals in time delay domain to accomplish the parallel acquisition. Each Doppler frequency bin contains correlation outputs from distinct code stages. As a consequence, 3-D plane grid representation is used to construct Doppler-code frequency bins. Before the local PRN code correlation procedure begins, the received signal is digitized and the carrier frequency is removed. The signal is measured using undetermined frequency and phase offsets, and the correlation output is assessed using a specified threshold. The incoming analog signal is collected by ADC, which subsequently transforms it into a digital signal. The digitized signal is mixed with a cosine signal produced by a cosine generator, as described by equation (1).

$$X_1[n] = s(n)Cos[2\pi(FBB + FD)n + \varphi 2] \quad (1)$$

$$s(n) = c(n)D(n)Cos(w_{IF}n) + e(n) \quad (2)$$

Where s(n) is the received signal as given in the equation (2) and c(n) gives PRN code replica, e(n) is the noise within units of 1/ fs and n determines whether the signal is discrete in time since it is sampled with the ADC at the fs sampling frequency.

Simultaneously, it mixes with the 90-degree phase-shifted signals, i.e. the Sine signal, as represented in equation (3).

$$X_Q[n] = s(n)Sin[2\pi(FBB + FD)n + \varphi 2] \quad (3)$$

All of the signals in equations (1) and (3) are correlated with FFT and multiplexed with their conjugate. After computing its inverse, the modulus of the inverse equation is summed to obtain the signal. The block diagram of the parallel acquisition unit in the time domain is shown in Figure 2.

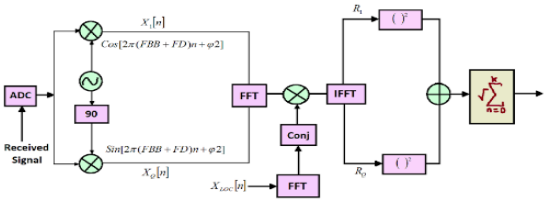


Fig2. Block diagram of an Acquisition unit

## 2.5 Tracking Unit

Once the acquisition is found to be effective, the satellites are visible at that moment. The visible satellite signal is then fine-tuned continually in terms of coding phase and Doppler frequency. The functioning diagram of the tracking device is shown in Fig 3. The satellites become visible once the purchase has been verified to be effective. The coding stage and Doppler frequency are then continually adjusted to the clear satellite signal in the following phase. PRN and carrier signal are the two local signals that are employed in the demodulation process, and they must match the

receiving signal perfectly. To make an exact copy, some feedback is required. The replica's feedback loop is called the carrier monitoring loop, while the code tracking loop is the feedback loop for replicating the precise PRN code. The carrier wave and the PRN code are removed from the received signal during tracking, leaving just a limited amount of noise level and navigation data.

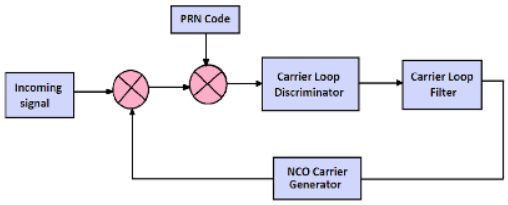


Fig3. Block diagram of acquisition unit

## 3 Algorithms for interference cancellations in Acquisition unit

One of the most difficult aspects of adaptive filtering is choosing an acceptable cost function [20]. MSE also known as mean square error is a popular CF, Cost Function because of Its ease, low computing burden, mathematical flexibility, circularity, and maximum efficiency when the noisy distribution presumption is Gaussian [21]. This criteria has been used to build numerous algorithms, including LMS, [22] Least Mean Square, variable step-size Least Mean Square, VSS-LMS, normalized Least Mean Square, NLMS [23] and variable step-size normalized Least Mean Square, VSS-NLMS. [24] However, in many real-world situations, the noise may be impulsive or non-Gaussian. The efficiency of MSE-based algorithms declines in these situations, and the algorithm deviates in certain cases [25].

Whenever the noise or the noisy signal has a luminous non-Gaussian distribution, the cost function ought to be a higher-order estimate of the error function [26]. The LMF, least mean fourth group of algorithms is one example of an algorithm that uses this characteristic. Nevertheless, its performance is hampered by the issue of instability. Least mean logarithmic square (LMLS) [27] method has similar convergence behavior to LMF but an improved stability greatly. In addition, a robust LMLS (R-LMLS) [28] method was introduced, which improves the LMLS algorithm's efficiency by offering resilience against impulsive sounds while simultaneously improving filter accuracy. The low order value of the error measured gives better resilience against the impulsive disturbances when the noisy signal tracks are heavily loaded in the tail of non-Gaussian distribution. [29]

$$y(n) = w^T(n)x(n) \tag{4}$$

$$x(n) = [x(n),....,x(n-M+1)]^T \tag{5}$$

$$w(n) = [w_0, w_1, w_2,....., w_{M-1}]^T \tag{6}$$

Equation (4) provides the model's output, when the model is an adaptive FIR filter. Here x(n) denotes the M-length tap delayed input signal vector, and w(n) denotes the model's adaptive weight vector mathematically as represented by equation (5) and (6) respectively for system identification issue.[30] The desired signal is represented by the equation (7) where v(n) is the background additive noisy signal and $w_0$ is the ideal weight vector.

$$d(n) = w_0^T(n)x(n) + v(n) \tag{7}$$

The difference of the desired signal and the ouput signal i.e equation (4) and (7) depicts the error of the signal as shown in equation (8).

$$e(n) = d(n) - y(n) \tag{8}$$

### 3.1 ASTA Algorithm

CF, Cost Function in the Arc-tangent Sign Algorithm is expressed the same as in the traditional sign algorithm, SA as given in equation (9).

$$\varsigma(n) = E\left[|e(n)|\right] \tag{9}$$

While corporating the above given traditional sign algorithm cost function with the arc-tangent framework and making use of it in the weight modification function, we get the arc-tangent sign method, which is represented in equation (10).

$$w(n+1) = w(n) + \mu \frac{sign[e(n)]x(n)}{1+\left[\gamma|e(n)|\right]^2} \tag{10}$$

The traditional SA is resistant against impulsive sounds, but its performance declines in a steady state. In addition to that, it has a sluggish convergence speed [31]. From the above equation (10), we can see that the weight update of ATSA has an additional term as compared to the standard SA. When this additional component approaches zero for high error values, as in the context of irrational disturbances, it offers an insignificant updation of weight, w(n) for larger disturbances [32]. In the same manner, for tiny values of error, the additional term associated with ASTA has a minor influence on the weight update function when it goes to one. In comparison to SA, this attribute renders the above algorithm rigorous against the non-Gaussian or non impulsive sounds.

### 3.2 ATLMS Algorithm

We acquire the arc-tangent least mean square algorithm, ATLMS by incorporating CF, cost functions as given by equation (11) of Mean Square Error, MSE which is based on the conventional LMS algorithm into the arc-tangent framework and applying the normalized weight update equation

$$\varsigma(n) = E\left[|e^2(n)|\right] \tag{11}$$

The weight upgrades of the ATLMS algorithm are given by equation (12). As explained in terms of the ATSA algorithm, [30] ATLMS is also dependent on the additional component present in equation (12) that enhances the robustness of the algorithm.

$$w(n+1) = w(n) + \mu \frac{e(n)x(n)}{1+\left[\gamma e^2(n)\right]^2} \tag{12}$$

LMS is the steepest descent method that tracks the gradient in the negative direction to the desired local minima at first. LMS is step sized that may be described as a direction factor for determining the negative descent pattern. The weight vector and step size are used to verify the convergence rate. To achieve optimal convergence speed and reduce message error, step size ought to be chosen small [33]. Among the most significant strength criterion for adaptive algorithms is the appropriate step size choosing. The changed filter coefficients are then used to estimate the output signal.

## 4 Simulation Analysis

This study explores the simulation findings on the basis of Galileo GNSS jamming and anti-jamming. The MATLAB program was used to execute all the simulations in this article. It can be visualized from the simulation that the results for anti-jamming using adaptive filters can be satisfactory in terms of Doppler frequency and code phase shift. Figure 4.(a) depicts the acquisition peak under standard circumstances with no jamming manipulations. The noise floor to peak maximum SNR is found to be 16.12 dB. As demonstrated in Figure 4.(b), the chirp jamming strategy has now been deployed such that the acquisition peak stays unnoticed. An array of spikes of varying heights is generated, and tracing the exact acquisition peak is very difficult.

The ground noise-to-peak ratio has been lowered to 4 dB as a result of the jamming, which is less than that of the peak detection limit for the Constant False Alarm Rate, CFAR algorithm. Then follows the noise decline or elimination of the components, which is represented in Fig 4.(c) and 4.(d) in order to recover the real signal. This is where the anti-jamming technology turns up to the play. To get the same result, we use the ATSA algorithm in Fig 4.(c) and ATLMS algorithm in Fig 4.(d) at the receiver end.

Although some because nothing in the planet is flawless, data do gets lost, we are able to recover the majority of the real or original captured signal with a noise floor to the highest peak-ratio of 14.515 dB using Arctangent Sign Algorithm (ATSA) and 15.084 dB using Arctangent Least Mean Square (ATLMS) Algorithm. Comparing the two figures (c) and (d) we can conclude that the ATLMS technique has the capability of retrieving a major portion of the original signal. As a result, it may be employed in any GNSS application, such as tracking mechanisms, moisture content determination, and ionosphere monitoring.

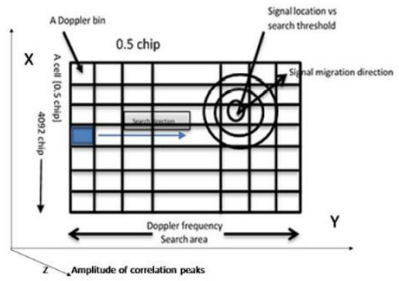


Fig 4. Finding peak location in Doppler frequency (125 Hz spacing) in Y axis and Code phase delay (0.5 chip: 1023*6/(12*1.023E6) = 0.5 msec)

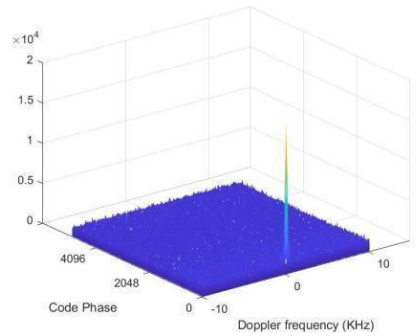


Fig. 5. (a) Peak acquisition without jamming in normal conditions;

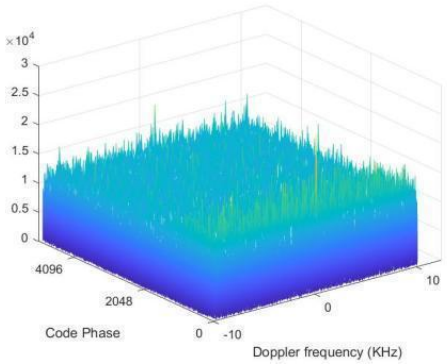


Fig. 5. (b) Peak acquisition after Chirp Jamming i.e the peak is undetected;

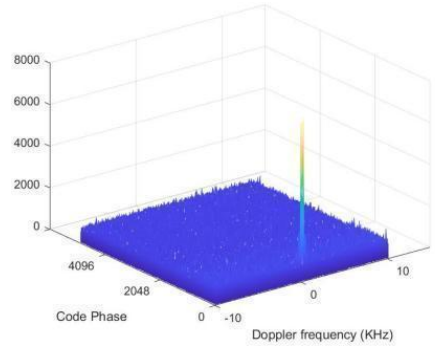


Fig. 5. (c) ATSA Anti-Jamming Technique to retrieve the signal for the Acquiring the Peak.

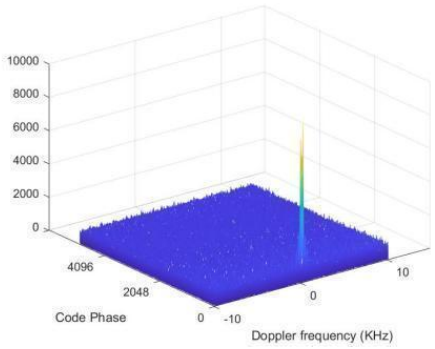


Fig. 5. (d) ATLMS Anti-Jamming Technique to retrieve the signal for the Acquiring the Peak.

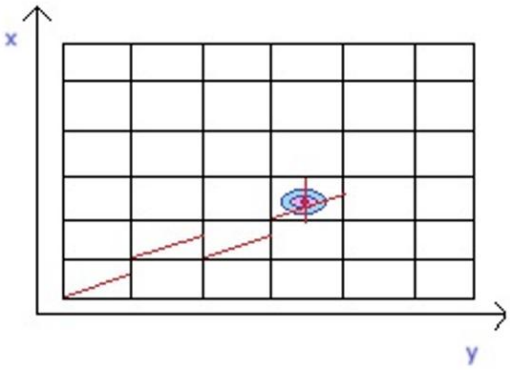


Fig. 6. Simplex transportation method using Vogel's method for peak find.

Table.1 Algorithms vs Peak to Noise Bed Ratio

| Signal Properties | **Peak to Noise Bed Ratio** | | | | | | |
|---|---|---|---|---|---|---|---|
| Signal to Noise Ratio | SNR (-11.02 dB) | SNR (-15.02 dB) | SNR (-20.02 dB) | SNR (-25.02 dB) | SNR (-30.52 dB) | SNR (-35.52 dB) | SNR (-36.02 dB) |
| Arc-Tangent Least Mean Squares | 15.0751 | 14.8048 | 14.2846 | 12.9123 | Not detected | Not detected | Not detected |
| Arc-Tangent Sign Algorithm | 14.2902 | 14.573 | 14.0131 | 13.37 | 10.7145 | Not detected | Not detected |
| Normalized Least Mean Squares | 12.3764 | 12.3338 | 11.9096 | 11.7423 | 10.896 | 9.8602 | 9.7954 |
| Recursive Least Squares | 15.3645 | 15.2295 | 14.8451 | 14.1101 | 12.9425 | 12.0268 | 11.9626 |

Table.2 Different Algorithms vs Time Elapsed

| | **Time Elapsed (in Seconds)** | | | | | | |
|---|---|---|---|---|---|---|---|
| Signal to Noise Ratio | SNR (-11.02 dB) | SNR (-15.02 dB) | SNR (-20.02 dB) | SNR (-25.02 dB) | SNR (-30.52 dB) | SNR (-35.52 dB) | SNR (-36.02 dB) |
| Arc-Tangent Least Mean Squares | 0.166122 | 0.115352 | 0.107095 | 0.117601 | Not detected | Not detecte | Not detected |
| Arc-Tangent Sign Algorithm | 0.138732 | 0.14846 | 0.127195 | 0.127169 | 0.137675 | Not detected | Not detected |
| Normalized Least Mean Squares | 0.093179 | 0.094452 | 0.122995 | 0.086072 | 0.097106 | 0.115826 | 0.099197 |
| Recursive Least Squares | 0.105668 | 0.10575 | 0.093637 | 0.104874 | 0.096338 | 0.09722 | 0.097239 |

## 5. Conclusion

In today's world, the GNSS has multiple applications in domains such as real-time tracking, military domain and many more. GALILEO GNSS is both the world's newest and most sophisticated GNSS at the moment. According to the speed and accuracy, it has significant benefits over standard GPS and GLONASS systems. [1] As a result, it's of no surprise that it will overtake others as the most extensively used navigation system in the upcoming times. According to the authors' conclusions, this study primarily focuses on the deployment of chirp jammers and a few algorithms for anti-jamming of GALILEO GNSS. [5] The complete design technique and outcomes have been thoroughly examined in the preceding sections. It has been discovered that chirp jammers are so effective at jamming that the original data signal is virtually recovered utilizing the ATSA, and ATLMS algorithms at the transceiver when the noise floor to highest peak point drops underneath the CFAR threshold point of peak detection. The proposal presented in the arctangent framework, a novel robust cost function framework. A series of resilient adaptive algorithms based on the novel framework have indeed been built by embedding conventional cost functions within an arctangent framework. As a result, the GNSS system may be widely employed in real-world scenarios, primarily for military purposes. The simplex transportation method using Vogel’s approximation or peak approximation function at MATLAB FINDPEAKS.m are used in peak location.

The inter-operability between GPS L5 signal and GALILEO E5a/ E5b signal, in terms of acquisition, tracking and data demodulation thresholds, which depend upon SNR, are computed in [34, 35]. It is to be noted that, we can use ambiguity function of GNSS signal, with code delay Doppler frequency plane as described in [36] and instead of using fixed threshold, we can dynamically choose the threshold value which does not rely on the C/N0 value or noise distribution [37].

## References

[1] Alkan, R. M., Karaman, H., & Sahin, M. GPS, GALILEO and GLONASS satellite navigation systems & amp; GPS modernization.

[2] Dutta, P., Halder, T., Banerjee, S., Basak, A., Nanda, S., & Chakravarty, D. (2022). Analysis of jamming and anti jamming techniques for Galileo GNSS. *Materials Today: Proceedings*, *58*, 489-495.

[3] Hu, H., & Wei, N. (2009, December). A study of GPS jamming and anti-jamming. In *2009 2nd international conference on power electronics and intelligent transportation system (PEITS)* (Vol. 1, pp. 388-391). IEEE.

[4] Yao, Z., Lu, M., & Feng, Z. (2009). Unambiguous technique for multiplexed binary offset carrier modulated signals tracking. *IEEE Signal Processing Letters*, *16*(7), 608-611.

[5] Tom, S. Perspective on GNSS compatibility and interoperability. In *Second meeting of the International Committee on Global Navigation Satellite System* (pp. 1025-1056).

[6] Julien, O., Macabiau, C., Cannon, M. E., & Lachapelle, G. (2007). ASPeCT: Unambiguous sine-BOC (n, n) acquisition/tracking technique for navigation applications. *IEEE Transactions on Aerospace and Electronic Systems*, *43*(1), 150-162.

[7] Yao, Z. (2008, September). A new unambiguous tracking technique for sine-BOC (2n, n) signals. In *Proceedings of the 21st International Technical Meeting of the Satellite Division of The Institute of Navigation (ION GNSS 2008)* (pp. 1490-1496).

[8] Heiries, V., Àvila-Rodriguez, J. À., Irsigler, M., Hein, G. W., Rebeyrol, E., & Roviras, D. (2005, September). Acquisition performance analysis of composite signals for the L1 OS optimized signal. In *Proceedings of the 18th International Technical Meeting of the Satellite Division of the Institute of Navigation (ION GNSS 2005)* (pp. 877-889).

[9] Lee, Y., Chong, D., Song, I., Kim, S. Y., Jee, G. I., & Yoon, S. (2012). Cancellation of correlation side-peaks for unambiguous BOC signal tracking. *IEEE Communications Letters*, *16*(5), 569-572.

[10] Hein, G. W., Avila-Rodriguez, J. A., Wallner, S., Pratt, A. R., Owen, J., Issler, J. L., ... & Stansell, T. A. (2006, April). MBOC: the new optimized spreading modulation recommended for GALILEO L1 OS and GPS L1C. In *Proceedings of IEEE/ION PLANS 2006* (pp. 883-892).

[11] Kaplan, E. D., & Hegarty, C. (Eds.). (2017). *Understanding GPS/GNSS: principles and applications*. Artech house.

[12] Hein, G. W., Avila-Rodriguez, J. A., Wallner, S., Pratt, A. R., Owen, J., Issler, J. L., ... & Stansell, T. A. (2006, April). MBOC: the new optimized spreading modulation recommended for GALILEO L1 OS and GPS L1C. In *Proceedings of IEEE/ION PLANS 2006* (pp. 883-892).

[13] Arvizu, J. M. C., & Cruz, A. J. A. (2011, November). GNSS receiver based on a SDR architecture using FPGA devices. In *2011 IEEE Electronics, Robotics and Automotive Mechanics Conference* (pp. 383-388). IEEE.

[14] Samama, N. (2008). *Global positioning: Technologies and performance*. John Wiley & Sons.

[15] Brown, A.K., and Thompson, N., (2010). Dynamically reconfigurable software defifined radio for gnss applications. Technical report, DTIC Document.

[16] Jin, T., Wang, Y., Shi, L., & Zhang, H. (2008, October). Software defined radio GNSS receiver design over single DSP platform. In *2008 4th International Conference on Wireless Communications, Networking and Mobile Computing* (pp. 1-4). IEEE.

[17] Hurskainen, H., Simona Lohan, E., Hu, X., Raasakka, J., & Nurmi, J. (2008). Multiple gate delay tracking structures for GNSS signals and their evaluation with Simulink, SystemC, and VHDL. *International Journal of Navigation and Observation*, *2008*(1), 785695.

[18] Ries, L., Issler, J. L., Julien, O., & Macabiau, C. (2012). *U.S. Patent No. 8,094,071*. Washington, DC: U.S. Patent and Trademark Office.

[19] Betz, J. W., Hegarty, C. J., & Rushanan, J. J. (2008). *U.S. Patent Application No. 11/785,571*.

[20] Lohan, E. S., Burian, A., & Renfors, M. (2008). Low-complexity unambiguous acquisition methods for BOC-modulated CDMA signals. *International Journal of Satellite Communications and Networking*, *26*(6), 503-522.

[21] P.S. Diniz, *Adaptive Filtering*. Springer, 2020.

[22] Peng, S., Ser, W., Chen, B., Sun, L., & Lin, Z. (2018). Robust constrained adaptive filtering under minimum error entropy criterion. *IEEE Transactions on Circuits and Systems II: Express Briefs*, *65*(8), 1119-1123.

[23] Chen, B., Xing, L., Zhao, H., Zheng, N., & Prı, J. C. (2016). Generalized correntropy for robust adaptive filtering. *IEEE Transactions on Signal Processing*, *64*(13), 3376-3387.

[24] He, H., Chen, J., Benesty, J., & Yu, Y. (2021, June). Robust recursive least M-estimate adaptive filter for the identification of low-rank acoustic systems. In *ICASSP 2021-2021 IEEE International Conference on Acoustics, Speech and Signal Processing (ICASSP)* (pp. 940-944). IEEE.

[25] Shi, L., & Lin, Y. (2014). Convex combination of adaptive filters under the maximum correntropy criterion in impulsive interference. *IEEE Signal Processing Letters*, *21*(11), 1385-1388.

[26] Sayin, M. O., Vanli, N. D., & Kozat, S. S. (2014). A novel family of adaptive filtering algorithms based on the logarithmic cost. *IEEE Transactions on signal processing*, *62*(17), 4411-4424.

[27] Xiong, K., & Wang, S. (2019). Robust least mean logarithmic square adaptive filtering algorithms. *Journal of the Franklin Institute*, *356*(1), 654-674.

[28] Huang, Y., Zhang, Y., Shi, P., Wu, Z., Qian, J., & Chambers, J. A. (2017). Robust Kalman filters based on Gaussian scale mixture distributions with application to target tracking. *IEEE Transactions on Systems, Man, and Cybernetics: Systems*, *49*(10), 2082-2096.

[29] Wang, S., Wang, W., Xiong, K., Iu, H. H., & Tse, C. K. (2019). Logarithmic hyperbolic cosine adaptive filter and its performance analysis. *IEEE Transactions on Systems, Man, and Cybernetics: Systems*, *51*(4), 2512-2524.

[30] Benesty, J., Paleologu, C., & Ciochina, S. (2010). On regularization in adaptive filtering. *IEEE Transactions on audio, speech, and language processing*, *19*(6), 1734-1742.

[31] Chen, B., Xing, L., Zhao, H., Zheng, N., & Prı, J. C. (2016). Generalized correntropy for robust adaptive filtering. *IEEE Transactions on Signal Processing*, *64*(13), 3376-3387.

[32] Kumar, K., Pandey, R., Bora, S. S., & George, N. V. (2021). A robust family of algorithms for adaptive filtering based on

the arctangent framework. *IEEE Transactions on Circuits and Systems II: Express Briefs*, *69*(3), 1967-1971.

[33] Gao, W., & Liu, S. (2011). Improved artificial bee colony algorithm for global optimization. *Information Processing Letters*, *111*(17), 871-882.

[34] Pajala, E., Lohan, E. S., & Renfors, M. (2005, July). CFAR detectors for hybrid-search acquisition of Galileo signals. In *CDROM Proc. of ENC-GNSS*.

[35] Brahim, F., Chonavel, T., & Rabaste, O. (2008, May). An MCMC algorithm for BOC and AltBOC signaling acquisition in multipath environments. In *2008 IEEE/ION Position, Location and Navigation Symposium* (pp. 424-432). IEEE.

[36] Bastide, F., Julien, O., Macabiau, C., & Roturier, B. (2002, September). Analysis of L5/E5 acquisition, tracking and data demodulation thresholds. In *Proceedings of the 15th International Technical Meeting of the Satellite Division of The Institute of Navigation (ION GPS 2002)* (pp. 2196-2207).

[37] De Wilde, W., Sleewaegen, J. M., Simsky, A., Vandewiele, C., Peeters, E., Grauwen, J., & Boon, F. (2006, May). New fast signal acquisition unit for GPS/Galileo receivers. In *Proceedings of ENC GNSS*.

[38] Dai, L., Wang, Z., Wang, J., & Song, J. (2010, September). Joint code acquisition and Doppler frequency shift estimation for GPS signals. In *2010 IEEE 72nd Vehicular Technology Conference-Fall* (pp. 1-5). IEEE.